CKLF1, transcriptionally activated by FOXC1, promotes hypoxia/reoxygenation-induced oxidative stress and inflammation in H9c2 cells by NLRP3 inflammasome activation

YINFENG JIA and JIANSHENG PAN

Department of Cardiovascular Medicine, The Second People's Hospital of Yueqing, Wenzhou, Zhejiang 325608, P.R. China

Received July 12, 2023; Accepted August 11, 2023

DOI: 10.3892/etm.2023.12347

Abstract. Myocardial ischemia/reperfusion (I/R) injury is a clinical challenge in the treatment of ischemic heart disease. The present study aimed to establish a hypoxia/reoxygenation (H/R)-induced H9c2 cell model to explore the role and mechanism of chemokine-like factor 1 (CKLF1) in myocardial I/R injury. First, CKLF1 expression was measured in H/R-induced H9c2 cells by reverse transcription-quantitative PCR and western blotting. Subsequently, after CKLF1 silencing, cell viability and apoptosis were evaluated by Cell Counting Kit-8 assay and flow cytometry. In addition, 2,7-dichlorodihydrofluorescein diacetate staining was used to assess the levels of cellular reactive oxygen species. Additionally, the levels of superoxide dismutase, glutathione peroxidase and malondialdehyde, and the contents of inflammatory factors IL-6, IL-1β and TNF-α were detected using corresponding commercially available kits. Western blotting was used to examine the expression levels of proteins involved in the NOD-like receptor family, pyrin domain containing 3 (NLRP3) inflammasome. The JASPAR database predicted that forkhead box protein C1 (FOXC1) would bind to the CKLF1 promoter region, and dual luciferase and chromatin immunoprecipitation assays were performed to verify it. Subsequently, FOXC1 overexpression and CKLF1 silencing were used to clarify the regulatory mechanism of FOXC1 on CKLF1 in H/R-induced H9c2 cells. The results revealed that CKLF1 expression was markedly enhanced in H/R-stimulated H9c2 cells. CKLF1 knockdown enhanced the viability and inhibited the apoptosis of H9c2 cells exposed to H/R. Moreover, the oxidative stress and inflammation induced by H/R were alleviated following CKLF1 silencing. CKLF1 knockdown also inhibited NLRP3 inflammasome activation. Furthermore, FOXC1 bound to the CKLF1 promoter region to upregulate CKLF1 expression, and FOXC1 overexpression alleviated the effects of CKLF1 knockdown on H9c2 cell damage induced by H/R via activation of the NLRP3 inflammasome. In conclusion, CKLF1 transcriptionally activated by FOXC1 may promote H/R-induced oxidative stress and inflammation in H9c2 cells via NLRP3 inflammasome activation.

Correspondence to: Dr Jiansheng Pan, Department of Cardiovascular Medicine, The Second People's Hospital of Yueqing, 322 Xinfeng Road, Hongqiao Town, Yueqing, Wenzhou, Zhejiang 325608, P.R. China
E-mail: panjiansheng860524@163.com

Key words: myocardial ischemia/reperfusion, oxidative stress, inflammation, apoptosis, NLRP3 inflammasome

Introduction

Acute myocardial infarction (AMI), which has been reported to be a main cause of death and disability worldwide, is a severe cardiovascular disease that results from the acute loss of viable myocardium due to hypoxia (1). Restoring blood flow to the ischemic area, namely reperfusion therapy, is the most common treatment for AMI, but it can sometimes abnormally aggravate myocardial injury, myocardial cell death and cause additional cardiac dysfunction in clinical practice in a process known as myocardial ischemia/reperfusion (I/R) injury (2). As a complex pathophysiological process during hypoxia and subsequent reperfusion, myocardial I/R has been reported to be promoted by oxidative stress radicals, inflammation and apoptosis in previous studies (3-5). However, the exact molecular mechanism remains unknown. Therefore, clarifying the mechanisms underlying the progression of myocardial I/R injury is necessary for identifying new therapeutic strategies and medicines.

Chemokine-like factor 1 (CKLF1) is a member of the CKLF protein family that has multiple biological functions, including chemotactic activities, inducing cell growth in multiple organs, and regulating vascular smooth muscle cell migration and proliferation after vascular injury (6-8). An increasing number of studies has validated the relationship between CKLF1 and ischemic disease. For example, CKLF1 aggravates early focal cerebral ischemic injury by regulating the polarization of microglia/macrophages to M1 type (9). Conversely, by promoting energy metabolism and inhibiting apoptosis, CKLF1 knockdown improves focal cerebral ischemia (10). Furthermore, IMM-H004 can downregulate the expression of CKLF1 to restrain activation of the NOD-like receptor family, pyrin domain containing 3 (NLRP3) inflammasome and the subsequent inflammatory reaction, ultimately protecting the ischemic brain (11). In addition, CKLF1 has been reported to be upregulated during hepatic

I/R, and CKLF1 inhibition can reduce neutrophil infiltration and decrease the inflammatory response to alleviate hepatic I/R injury (12). However, the role of CKLF1 in myocardial I/R injury has rarely been studied (13,14). The JASPAR database (https://jaspar.genereg.net/) indicated the putative forkhead box protein C1 (FOXC1)-binding site on the CKLF1 promoter. A previous study suggested that FOXC1 is a hypoxia-activated transcription factor that can promote lung cancer cell growth (15). Of note, FOXC1 can be induced to promote the inflammatory response and cell damage during myocardial ischemia (16). Therefore, the present study focused on whether CKLF1 could be transcriptionally activated by the transcription factor FOXC1 to participate in the progression of myocardial I/R.

In the present study, the hypoxia/reoxygenation (H/R)-induced H9c2 rat cardiomyoblast cell injury model was established to mimic myocardial I/R injury *in vitro* with the aim of investigating the effects of CKLF1 and FOXC1 on H/R injury from the perspectives of oxidative stress, inflammation and apoptosis. The present findings may provide information on the mechanisms underlying myocardial I/R and could aid the development of future therapies.

Materials and methods

Cell culture and H/R induction. The rat cardiomyoblast cell line H9c2 was obtained from The Cell Bank of Type Culture Collection of The Chinese Academy of Sciences. The cells were placed in a constant temperature incubator at 37˚C and 5% CO_2, and were maintained in DMEM (Gibco; Thermo Fisher Scientific, Inc.) supplemented with 10% fetal bovine serum (HyClone; Cytiva). To simulate myocardial I/R *in vitro*, H9c2 cells at 80% confluence were transferred to serum- and glucose-free DMEM, and were cultivated in a hypoxic atmosphere of 0.1% O_2, 95% N_2 and 5% CO_2 for 6 h. Subsequently, the cells were maintained in the incubator with normal DMEM under normoxic conditions in the presence of 95% air and 5% CO_2 for 12 h for reoxygenation (17,18). H9c2 cells in the control group were cultured under normal culture conditions.

Transfection. For transfection, CKLF1 small interfering RNAs (siRNAs) (si-CKLF1#1 sense, 5'-GTCTTGACAAGA CAATGAGATCT-3', antisense, 5'-AGATCTCATTGTCTT GTCAAGAC-3'; si-CKLF1#2 sense, 5'-GCCTTTGCTTGA TGTTATCAACT-3', antisense, 5'-AGTTGATAACATCAA GCAAAGGC-3'), negative control siRNA (si-NC sense, 5'-CCTTATGTACGTTGATTCAGTACAA-3', antisense 5'-TTGTACTGAATCAACGTACATAAGG-3'), FOXC1 pcDNA3.1 plasmid (Oe-FOXC1) and empty vector (Oe-NC) were synthesized by Shanghai GeneChem Co., Ltd. H9c2 cells at the logarithmic phase were seeded in a 6-well plate ($1x10^5$ cells/well) and were incubated at 37˚C until they reached 80% confluence. Subsequently, 100 nM of recombinants were transfected into H9c2 cells at 37˚C for 48 h using Lipofectamine® 3000 (Invitrogen; Thermo Fisher Scientific, Inc.) according to the manufacturer's protocol. After 48 h, cells were collected and further experiments were performed. For H9c2 cells both subjected to H/R stimulation and co-transfection with si-CKLF1 and Oe-FOXC1, cells were pre-transfected for 48 h and then received H/R stimulation.

Cell viability assay. H9c2 cells were plated into a 96-well plate at a density of $1x10^4$ cells/well. Following H/R stimulation and indicated transfection, 10 μl Cell Counting Kit-8 (CCK-8) solution (Sangon Biotech Co., Ltd.) was added to each well and incubated for 3 h at 37˚C. The absorbance was detected at a wavelength of 450 nm using a microplate reader (BioTek Instruments, Inc.) to evaluate the viability of H9c2 cells.

Flow cytometric analysis. The apoptotic rate of H9c2 cells was determined following H/R stimulation and indicated transfection using an Annexin V-fluorescein isothiocyanate (FITC) kit (Shanghai GeneChem Co., Ltd.) according to the manufacturer's instructions. H9c2 cells were obtained and resuspended in 500 μl binding buffer. Subsequently, 100 μl cell suspension was transferred to a tube, to which 5 μl Annexin V-FITC and 10 μl propidium iodide was added. The mixture was incubated at room temperature for 5 min in dark. Finally, treated cells were analyzed using a flow cytometer (FACSCalibur; BD Biosciences) and Flowjo vX.0.7 software (FlowJo LLC) was used. Apoptotic cells were counted and expressed as a percentage of the total cell count.

Measurement of caspase 3 activity. Caspase 3 activity was measured using a caspase 3 colorimetric assay kit (cat. no. C1115; Beyotime Institute of Biotechnology) according to the manufacturer's guidelines. H9c2 cells were lysed in RIPA lysis buffer (cat. no. P0013B; Beyotime Institute of Biotechnology) and the lysates were centrifuged at 12,000 x g for 10 min at 4˚C. Cell lysates were then incubated with caspase 3 substrate (Ac-DEVD-pNA) for 2 h at 37˚C in the dark. The relative fluorescence was detected at 450 nm using a fluorescence plate reader.

Evaluation of intracellular reactive oxygen species (ROS). The measurement of intracellular ROS production was performed using the ROS assay kit (cat. no. S0033S; Beyotime Institute of Biotechnology) using the fluorescent probe 2,7-dichlorodihydrofluorescein diacetate (DCFH-DA). Following transfection and/or H/R treatment, H9c2 cells were incubated with 10 μmol/l DCFH-DA for 20 min at 37˚C in the dark. After washing three times with PBS, the fluorescence intensity of cells in each group was detected using a fluorescence spectrophotometer with 488 nm excitation and 525 nm emission filters.

Detection of oxidative stress indicators. After H/R stimulation and indicated transfection, H9c2 cells were centrifuged at 1,500 x g for 10 min at 4˚C. The activities of superoxide dismutase (SOD) and glutathione peroxidase (GSH-Px), and the content of malondialdehyde (MDA) in the supernatant of H9c2 cells were tested using SOD assay kits (cat. no. S0086; Beyotime Institute of Biotechnology), GSH-Px assay kits (cat. no. A005-1-2; Nanjing Jiancheng Bioengineering Institute) and MDA assay kits (cat. no. A003-1-2; Nanjing Jiancheng Bioengineering Institute), respectively, according to the manufacturer's protocols. The optical density was measured using a microplate reader (BioTek Instruments, Inc.).

ELISA. After H/R stimulation and indicated transfection, H9c2 cells were centrifuged at 2.000 x g for 5 min at 4˚C. The levels of tumor necrosis factor-α (TNF-α), interleukin (IL)-6 and IL-1β in the culture supernatant were detected using ELISA kits for TNF-α (cat. no. F3768; Shanghai Westang Biotechnology Co., Ltd.), IL-6 (cat. no. F3743; Shanghai Westang Biotechnology Co., Ltd.) and IL-1β (cat. no. F3739; Shanghai Westang Biotechnology Co., Ltd.). All experimental procedures were conducted in accordance with the manufacturer's guidelines.

Reverse transcription-quantitative PCR (RT-qPCR). After H/R stimulation and indicated transfection, TRIzol® reagent (Invitrogen; Thermo Fisher Scientific, Inc.) was used to isolate total RNA from H9c2 cells according to the manufacturer's recommendations. cDNA was synthesized from total RNA using the Prime Script RT Reagent Kit with gDNA Eraser (Takara Biotechnology Ltd.) according to the manufacturer's instructions. qPCR was performed using SYBR Green master mix (Vazyme Biotech Co., Ltd.) and detected on an ABI Prism 7500 Sequence Detector (Applied Biosystems; Thermo Fisher Scientific, Inc.). The following thermocycling conditions were used for qPCR: 95˚C for 10 min; followed by 40 cycles of 95˚C for 10 sec and 60˚C for 60 sec. The following primer pairs were used for qPCR: CKLF1 forward, 5'-GTTGAAGTT GTTGCGCGAGT-3' and reverse, 5'-ATACGGTTCAGGGGC TTGTG-3'; FOXC1 forward, 5'-CTATCCAGAATGCCCCGG AC-3' and reverse, 5'-CGTACCGTTCTCCGTCTTGA-3'; GAPDH forward, 5'-GCATCTTCTTGTGCAGTGCC-3' and reverse, 5'-GATGGTGATGGGTTTCCCGT-3'. GAPDH was used as an internal reference and the $2^{-\Delta\Delta Cq}$ method (19) was used for the calculation of relative mRNA expression levels.

Western blot analysis. After H/R stimulation and indicated transfection, H9c2 cells were lysed in RIPA lysis buffer and the lysates were centrifuged at 12,000 x g for 10 min at 4˚C to obtain proteins. The protein concentration was determined using the bicinchoninic acid method. Equal amounts of protein (40 μg) were separated by SDS-PAGE on 10% gels and were then transferred to PVDF membranes. After blocking in 5% non-fat milk for 1 h at room temperature, the membranes were probed with primary antibodies overnight at 4˚C, followed by incubation with a HRP-conjugated secondary antibody (1:5,000; cat. no. 7074P2; Cell Signaling Technology, Inc.) at room temperature for 1 h. Immunoreactive proteins were visualized using an enhanced chemiluminescence kit (Thermo Fisher Scientific, Inc.) and gray intensity analysis was performed using ImageJ 1.8.0 software (National Institutes of Health). The expression levels of specific protein were normalized to GAPDH. The primary antibodies used in the present study were as follows: CKLF1 (1:1,000; cat. no. ab180512), Bcl-2 (1:2,000; cat. no. ab196495), NLRP3 (1:1,000; cat. no. ab263899), IL-18 (1:1,000; cat. no. ab191860) and IL-1β (1:1,000; cat. no. ab254360) (all from Abcam); gasdermin D N-terminal domain (GSDMD-N; 1:200; cat. no. DF13758; Affinity Biosciences); FOXC1 (1:1,000; cat. no. 8758S), Bax (1:1,000; cat. no. 14796S), cleaved PARP (1:1,000; cat. no. 94885S), PARP (1:1,000; cat. no. 9532T), caspase 1 (1:1,000; cat. no. 83383S) and GAPDH (1:1,000; cat. no. 5174T) (all from Cell Signaling Technology, Inc.).

Dual-luciferase reporter assay. Lipofectamine 3000 was used to co-transfect H9c2 cells with pGL3 vectors (Promega Corporation) containing the wild-type (WT) CKLF1 promoter sequence or the corresponding mutant CKLF1 promoter sequence, and Oe-FOXC1 or Oe-NC. A total of 48 h post-transfection, the firefly and *Renilla* luciferase activities were detected using a dual luciferase reporter assay system (Promega Corporation). The results obtained were normalized to *Renilla* luciferase activity.

Chromatin immunoprecipitation (ChIP) assay. The binding of FOXC1 to the CKLF1 promoter was validated using a ChIP assay kit (Beyotime Institute of Biotechnology). H9c2 cells were cross-linked with 1% formaldehyde solution for 10 min at 37˚C. Subsequently, the cross-linking reaction was quenched with 1.1 ml glycine solution (10X). DNA fragments were extracted by sonication using a 10 sec on and 10 sec off mode for 12 cycles at 4˚C and immunoprecipitated overnight at 4˚C with anti-FOXC1 (cat. no. ab227977; 1:50; Abcam) or negative control IgG antibodies (cat. no. 3423; 1:20; Cell Signaling Technology). The DNA isolated through ChIP reactions was evaluated using PCR as aforementioned.

Statistical analysis. GraphPad Prism 8.0 (Dotmatics) was used for statistical analysis. All experimental data are presented as the mean ± standard deviation from three experiments. The statistical significance between two groups was analyzed using an unpaired Student's t-test. One-way analysis of variance followed by Tukey's post-hoc test was performed to compare the data of multiple groups. $P<0.05$ was considered to indicate a statistically significant difference.

Results

CKLF1 is significantly upregulated in H/R-induced H9c2 cells. H9c2 cells exposed to H/R were used to establish an *in vitro* model of myocardial I/R injury. The results of RT-qPCR and western blotting indicated that H/R stimulation significantly upregulated the expression levels of CKLF1 compared with those in the control group (Fig. 1A and B). Subsequently, CKLF1 was silenced by transfection with siRNAs targeting CKLF1. Transfection with si-CKLF1#1 and si-CKLF1#2 led to significantly reduced CKLF1 expression when compared with the si-NC group (Fig. 1C and D). It is worthwhile to mention that si-CKLF1#1 was selected for subsequent experiments due to its better knockdown efficacy.

CKLF1 knockdown inhibits the apoptosis, oxidative stress and inflammation of H/R-induced H9c2 cells. Cell viability was evaluated using the CCK-8 assay in the presence or absence of H/R and si-CKLF1. As shown in Fig. 2A, H/R stimulation significantly decreased the viability of H9c2 cells when compared with the control group; however, this was reversed by CKLF1 silencing. In addition, the percentage of apoptotic H9c2 cells was significantly elevated following H/R induction, whereas CKLF1 knockdown partially alleviated the H/R-triggered increase in apoptosis (Fig. 2B). Furthermore, H9c2 cells under H/R conditions exhibited enhanced caspase 3 activity, upregulated Bax and cleaved PARP expression, and downregulated Bcl-2 expression compared with that in the

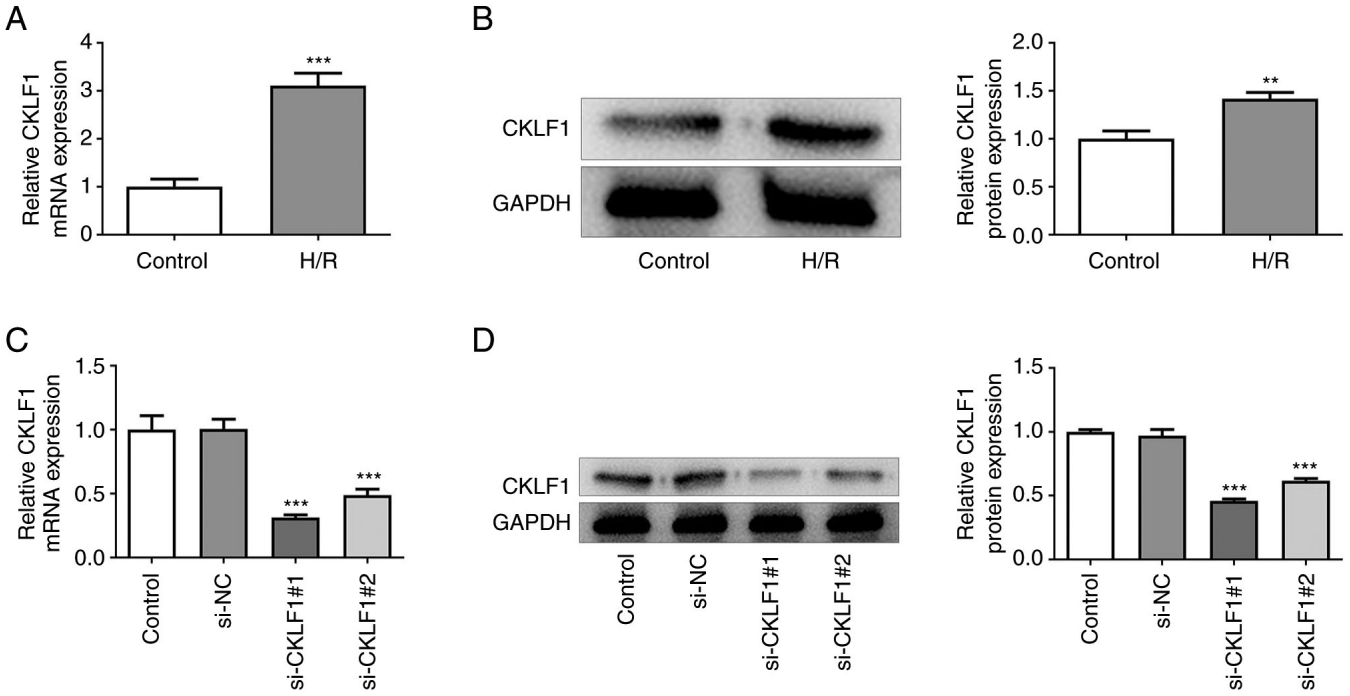

Figure 1. CKLF1 is significantly upregulated in H/R-induced H9c2 cells. CKLF1 mRNA and protein expression levels were detected in H/R-induced H9c2 cells using (A) RT-qPCR and (B) western blotting. **P<0.01, ***P<0.001 vs. control. CKLF1 mRNA and protein expression levels were detected in H9c2 cells post-transfection with si-CKLF1#1 and si-CKLF1#2 using (C) RT-qPCR and (D) western blotting. ***P<0.001 vs. si-NC. CKLF1, chemokine-like factor 1; H/R, hypoxia/reoxygenation; NC, negative control; RT-qPCR, reverse transcription-quantitative PCR; si, small interfering.

control group (Fig. 2C and D). However, CKLF1 knockdown attenuated the effects of H/R on the levels of caspase 3, Bax, cleaved PARP and Bcl-2. Subsequently, the levels of intracellular ROS were evaluated using DCFH-DA as a fluorescent probe in H9c2 cells exposed to H/R conditions. Markedly enhanced fluorescence intensity was observed in the H/R group compared with that in the control group (Fig. 2E). By contrast, CKLF1 silencing reduced the fluorescence intensity induced by H/R exposure. Furthermore, compared with that in the control group, H/R stimulation promoted the oxidative stress and inflammation of H9c2 cells, as evidenced by decreased SOD and GSH-Px activities, and increased MDA, TNF-α, IL-6 and IL-1β contents (Fig. 2F-K). Conversely, CKLF1 knockdown relieved the effects of H/R on the aforementioned oxidative stress and inflammation-related factors. These findings indicated that interference with CKLF1 inhibited the apoptosis, oxidative stress and inflammation of H/R-induced H9c2 cells.

CKLF1 knockdown suppresses NLRP3 inflammasome activation in H/R-induced H9c2 cells. The results of western blotting indicated that H/R led to the activation of NLRP3 inflammasome signaling by upregulating NLRP3, GSDMD-N, IL-18, IL-1β and caspase 1 expression (Fig. 3). Notably, CKLF1 knockdown contributed to the inactivation of NLRP3 inflammasome signaling compared with the H/R + si-NC group. These results suggested that CKLF1 silencing suppressed the oxidative stress, inflammation and NLRP3 inflammasome activation in H/R-induced H9c2 cells.

CKLF1 is transcriptionally activated by FOXC1 in H9c2 cells. The putative FOXC1-binding site on the CKLF1 promoter was identified using the JASPAR database (Fig. 4A). As shown in Fig. 4B and C, H9c2 cells under H/R conditions exhibited higher FOXC1 expression than that in the control group. Significantly elevated FOXC1 expression was observed after Oe-FOXC1 transfection (Fig. 4D and E). Moreover, FOXC1 overexpression significantly increased the luciferase activity in the CKLF1-WT group when compared with the Oe-NC group (Fig. 4F). ChIP assay also demonstrated that FOXC1 could bind with the CKLF1 promoter region (Fig. 4G). Furthermore, enhanced CKLF1 mRNA and protein expression levels were found in H9c2 cells in the Oe-FOXC1 group compared with the Oe-NC group (Fig. 4H and I). These results suggested that FOXC1 could transcriptionally activate CKLF1 and upregulate CKLF1 expression in H9c2 cells.

FOXC1 overexpression alleviates the inhibitory effects of CKLF1 knockdown on the apoptosis, oxidative stress and inflammation of H/R-induced H9c2 cells. FOXC1 was overexpressed in H9c2 cells to further explore whether FOXC1 transcriptionally activated CKLF1 to regulate H/R-induced damage. As shown in Fig. 5A, compared with in the H/R + si-CKLF1 + Oe-NC group, FOXC1 overexpression increased the apoptotic rate of H9c2 cells. In addition, FOXC1 overexpression elevated caspase 3 activity in H9c2 cells exposed to H/R; however, there was no significant difference when compared with the Oe-NC group (Fig. 5B). Furthermore, Bcl-2 expression was significantly decreased, and Bax and cleaved PARP expression was significantly increased in the H/R + si-CKLF1 + Oe-FOXC1 group when compared with the H/R + si-CKLF1 + Oe-NC group (Fig. 5C). As shown in Fig. 5D-G, FOXC1 overexpression in H9c2 cells transfected

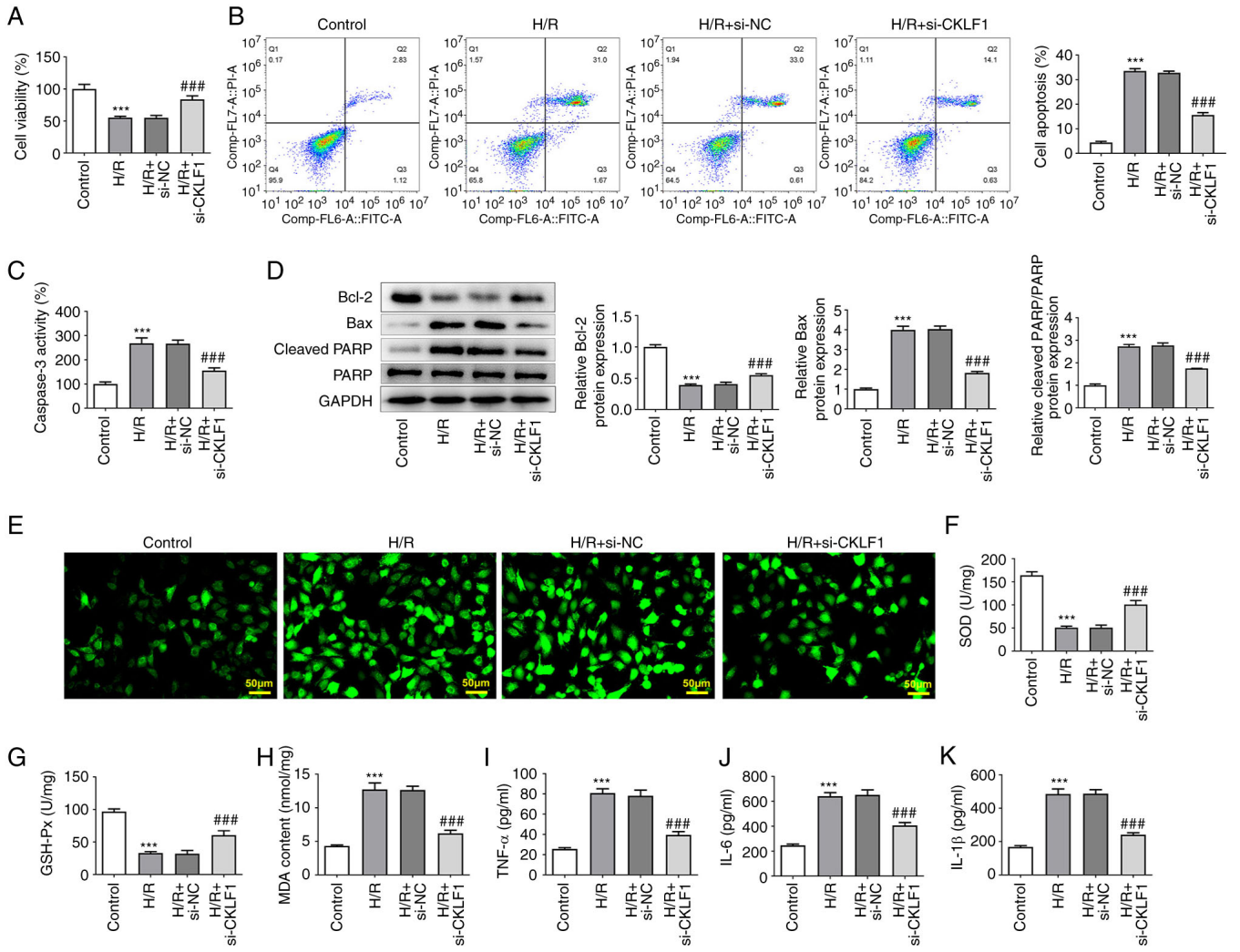

Figure 2. CKLF1 knockdown inhibits the apoptosis, oxidative stress and inflammation of H/R-induced H9c2 cells. (A) Cell viability was assessed by Cell Counting Kit-8 assay. (B) Apoptotic rate was measured by flow cytometric analysis. (C) Caspase 3 activity was detected using a caspase 3 colorimetric assay kit. (D) Western blotting was used to evaluate the expression levels of apoptosis-related proteins. (E) Intracellular reactive oxygen species were evaluated using 2,7-dichlorodihydrofluorescein diacetate as a fluorescent probe in H9c2 cells exposed to H/R conditions. The activities of (F) SOD and (G) GSH-Px, and the levels of (H) MDA, (I) TNF-α, (J) IL-6 and (K) IL-1β were examined using commercially available kits. ***P<0.001 vs. control; ###P<0.001 vs. H/R + si-NC. CKLF1, chemokine-like factor 1; GSH-Px, glutathione peroxidase; H/R, hypoxia/reoxygenation; IL, interleukin; MDA, malondialdehyde; NC, negative control; si, small interfering; SOD, superoxide dismutase; TNF-α, tumor necrosis factor-α.

with si-CKLF1 under H/R conditions exhibited elevated oxidative stress compared with that in the H/R + si-CKLF1 + Oe-NC group, as evidenced by the enhanced fluorescence intensity, increased MDA content, and decreased SOD and GSH-Px activities. Furthermore, the levels of inflammatory factors, including TNF-α, IL-6 and IL-1β, were significantly elevated in the H/R + si-CKLF1 + Oe-FOXC1 group compared with those in the H/R + si-CKLF1 + Oe-NC group (Fig. 5H-J). These findings indicated that FOXC1 overexpression partially reversed the inhibitory effects of CKLF1 knockdown on the apoptosis, oxidative stress and inflammation of H/R-induced H9c2 cells.

FOXC1 overexpression reverses the effects of CKLF1 knockdown on H/R-induced H9c2 cell damage via NLRP3 inflammasome signaling. Post-transfection with Oe-FOXC1 and si-CKLF1 in H9c2 cells exposed to H/R, the expression levels of proteins associated with NLRP3 inflammasome signaling were assessed by western blotting. As shown in Fig. 6, FOXC1 overexpression in H9c2 cells with CKLF1 knockdown led to markedly increased expression levels of NLRP3, GSDMD-N, IL-18, IL-1β and caspase 1. Taken together, these findings indicated that CKLF1 silencing, potentially mediated by FOXC1 downregulation, suppressed H/R-induced H9c2 cell damage by inhibiting NLRP3 inflammasome activation.

Discussion

Excessive apoptosis has long been considered a promoting factor for the pathological progression of myocardial I/R injury, and intervening in myocardial apoptosis is considered a promising approach in the prevention and reduction of myocardial I/R injury (20,21). Bcl-2 and Bax are two important proteins in the Bcl-2 protein family, which serve anti-apoptotic and pro-apoptotic roles in intrinsic apoptosis, respectively (22). PARP has a crucial role in DNA damage repair and loses its

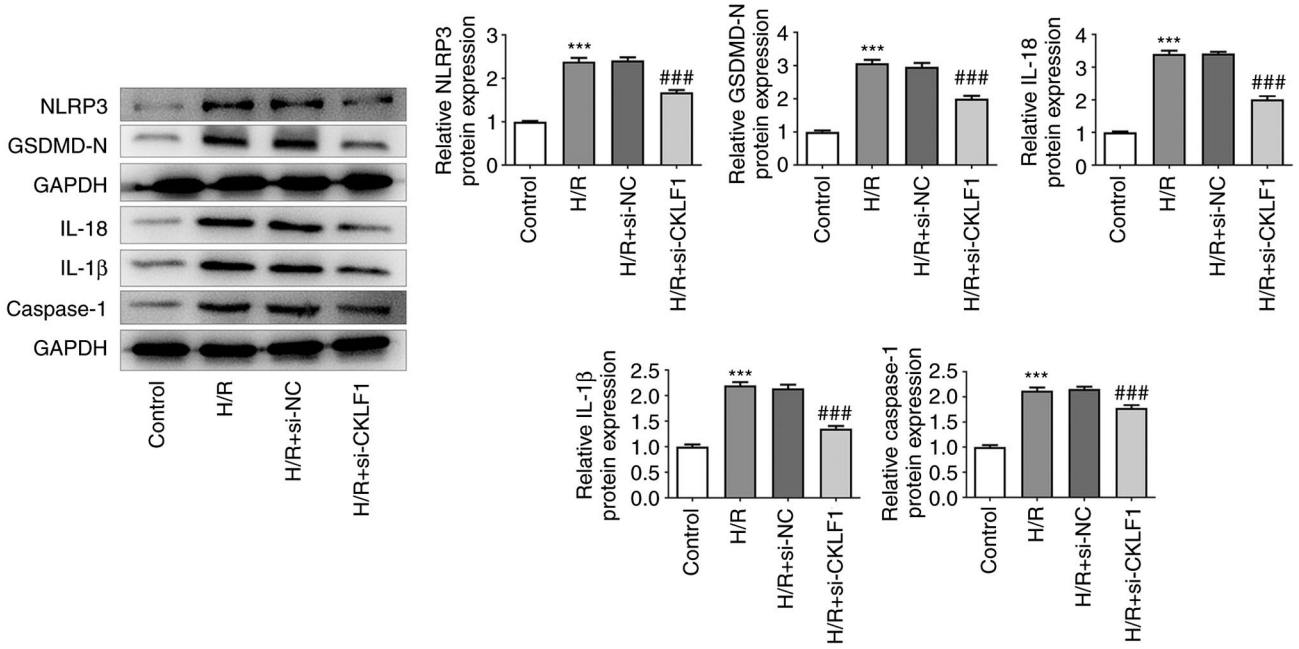

Figure 3. CKLF1 suppresses NLRP3 inflammasome activation in H/R-induced H9c2 cells. Proteins related to NLRP3 inflammasome signaling were assessed by western blotting. ***P<0.001 vs. control; ###P<0.001 vs. H/R + si-NC. CKLF1, chemokine-like factor 1; GSDMD-N, gasdermin D N-terminal domain; H/R, hypoxia/reoxygenation; IL, interleukin; NC, negative control; NLRP3, NOD-like receptor family, pyrin domain containing 3; si, small interfering.

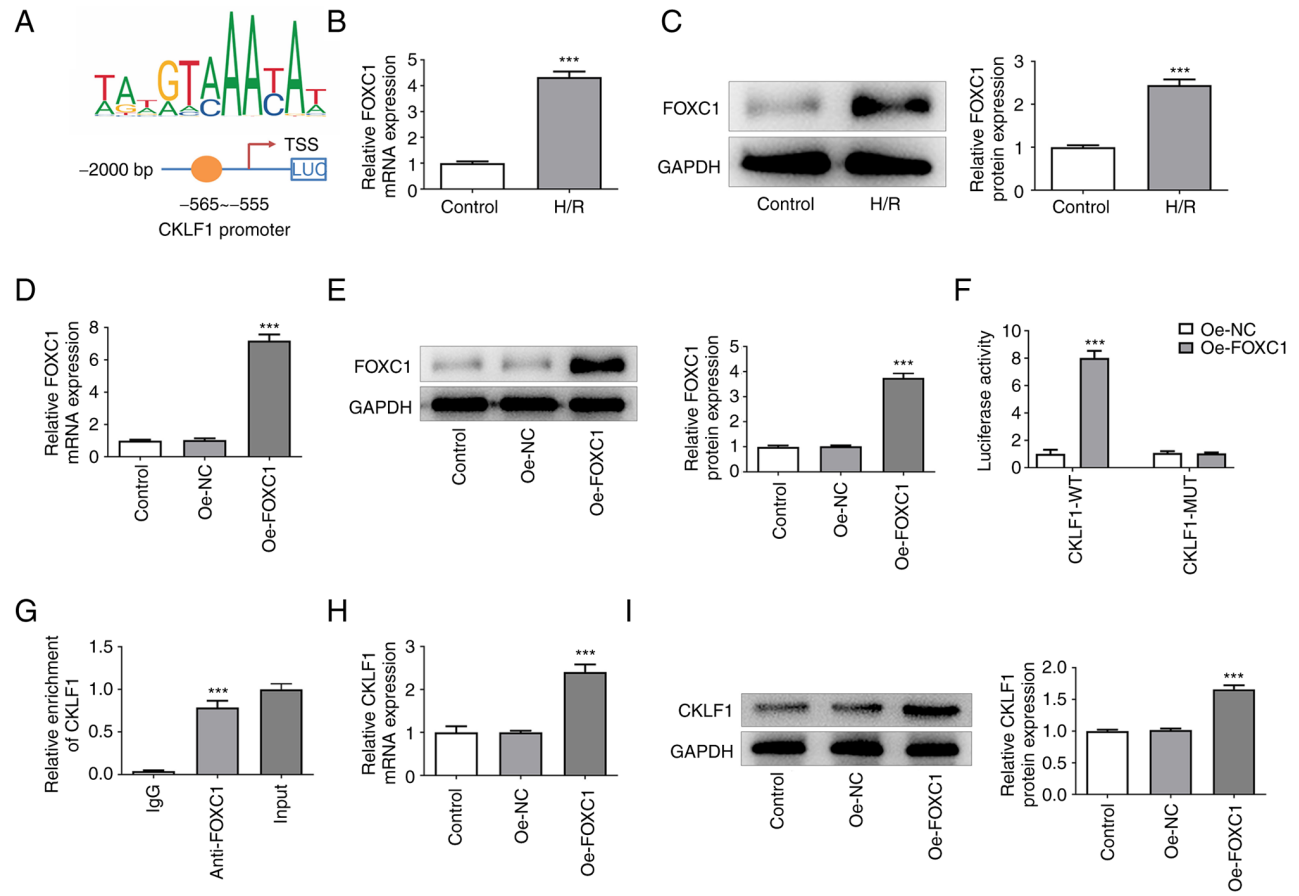

Figure 4. CKLF1 may be transcriptionally activated by FOXC1 in H9c2 cells. (A) Binding sites between FOXC1 and CKLF1. The expression of FOXC1 was detected in H/R-induced H9c2 cells using (B) RT-qPCR and (C) western blotting. ***P<0.001 vs. control. The expression of FOXC1 was detected in H9c2 cells post-transfection with OE-FOXC1 by (D) RT-qPCR and (E) western blotting. ***P<0.001 vs. Oe-NC. Binding between FOXC1 and CKLF1 promoter was confirmed by (F) dual-luciferase reporter assay and (G) chromatin immunoprecipitation assay. ***P<0.001 vs. IgG. The expression of CKLF1 was detected in H9c2 cells post-transfection with Oe-FOXC1 using (H) RT-qPCR and (I) western blotting. ***P<0.001 vs. Oe-NC. CKLF1, chemokine-like factor 1; FOXC1, forkhead box protein C1; H/R, hypoxia/reoxygenation; MUT, mutant; NC, negative control; OE, overexpression; RT-qPCR, reverse transcription-quantitative PCR; WT, wild-type.

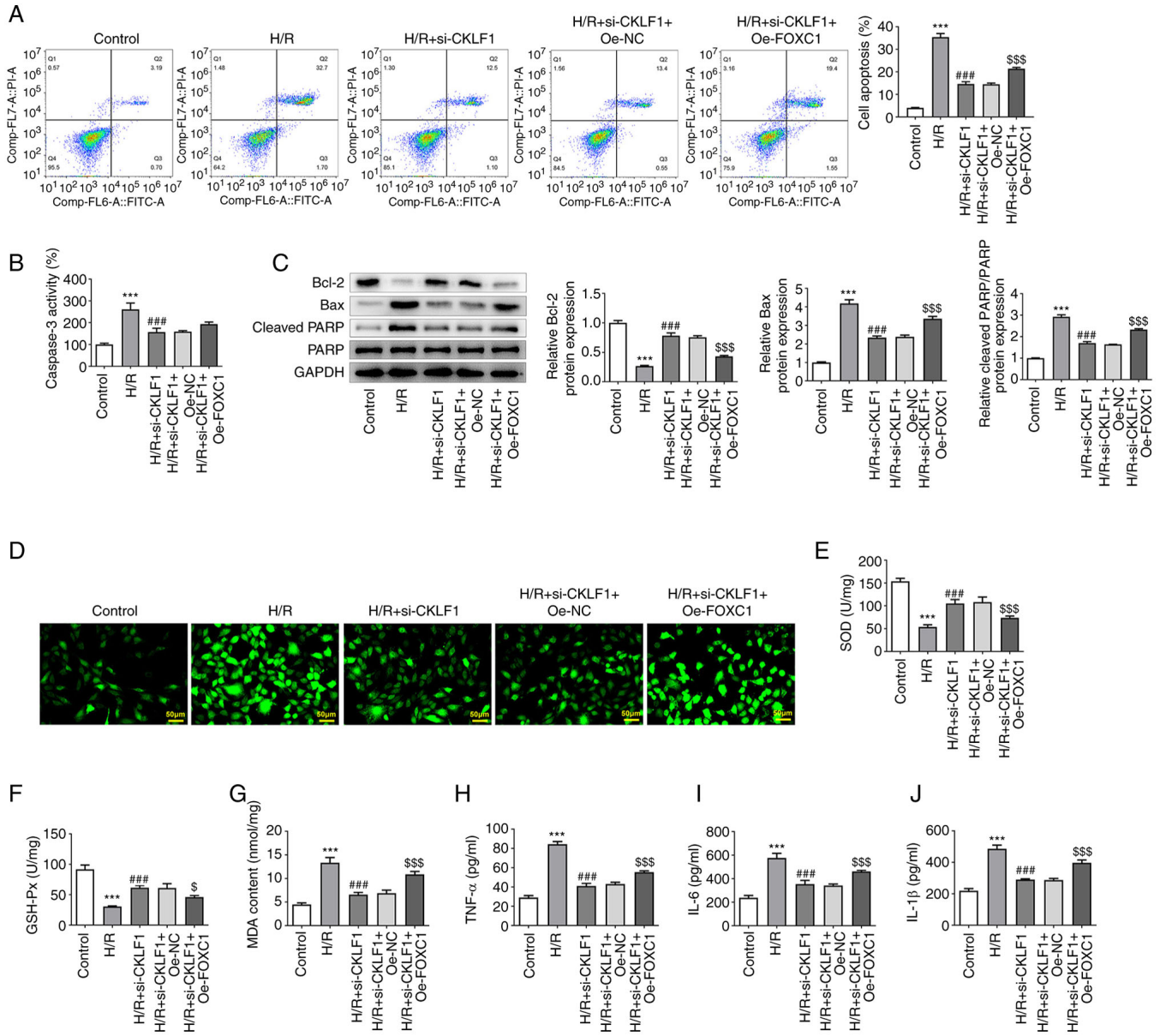

Figure 5. Oe-FOXC1 alleviates the inhibitory effects of CKLF1 knockdown on the apoptosis, oxidative stress and inflammation of H/R-induced H9c2 cells. (A) Cell apoptosis was measured using flow cytometry. (B) Caspase 3 activity was detected using a caspase 3 colorimetric assay kit. (C) Western blotting was used to evaluate the expression of apoptosis-related proteins. (D) Intracellular reactive oxygen species were evaluated using 2,7-dichlorodihydrofluorescein diacetate as a fluorescent probe. The activities of (E) SOD and (F) GSH-Px, and the levels of (G) MDA, (H) TNF-α, (I) IL-6 and (J) IL-1β were examined using commercially available kits. ***P<0.001 vs. control; $^{###}$P<0.001 vs. H/R; $^{\$}$P<0.05, $^{\$\$\$}$P<0.001 vs. H/R + si-CKLF1 + Oe-NC. CKLF1, chemokine-like factor 1; GSH-Px, glutathione peroxidase; FOXC1, forkhead box protein C1; H/R, hypoxia/reoxygenation; IL, interleukin; MDA, malondialdehyde; NC, negative control; OE, overexpression; si, small interfering; SOD, superoxide dismutase; TNF-α, tumor necrosis factor-α.

activity once PARP cleavage occurs, thus accelerating the apoptotic process (23). CKLF1, a novel chemokine discovered in 2001, is implicated in neuronal apoptosis following cerebral I/R, and CKLF1 inhibition has been shown to reduce Bax expression and elevate Bcl-2 expression in brain tissues (10). Furthermore, by attenuating CKLF1-mediated inflammation and apoptosis, hydroxytyrosol has been reported to exert protective effects on cisplatin-induced nephrotoxicity (24). In the present study, to the best of our knowledge, the role of CKLF1 in H/R-induced cardiomyocyte damage was explored for the first time. The results demonstrated that CKLF1 was highly expressed in H/R-stimulated H9c2 cells, and CKLF1 knockdown decreased the apoptotic rate of cells, accompanied by upregulated Bcl-2 expression, and downregulated Bax and cleaved PARP expression.

Cardiomyocytes are more susceptible to free radical damage because they contain fewer antioxidants and antioxidant enzymes, such as SOD and GSH-Px (25,26). MDA is the crucial indicator of membrane lipid peroxidation. Excessive ROS can cause extensive oxidative damage to cardiomyocytes, leading to loss of cell viability and myocardial stunning (27). Numerous studies have shown that ROS production is a hallmark of I/R injury, and myocardial injury caused by H/R is closely associated with ROS production and oxidative stress in cardiomyocytes (28,29). Inhibition of oxidative stress and reduction of ROS production can effectively alleviate

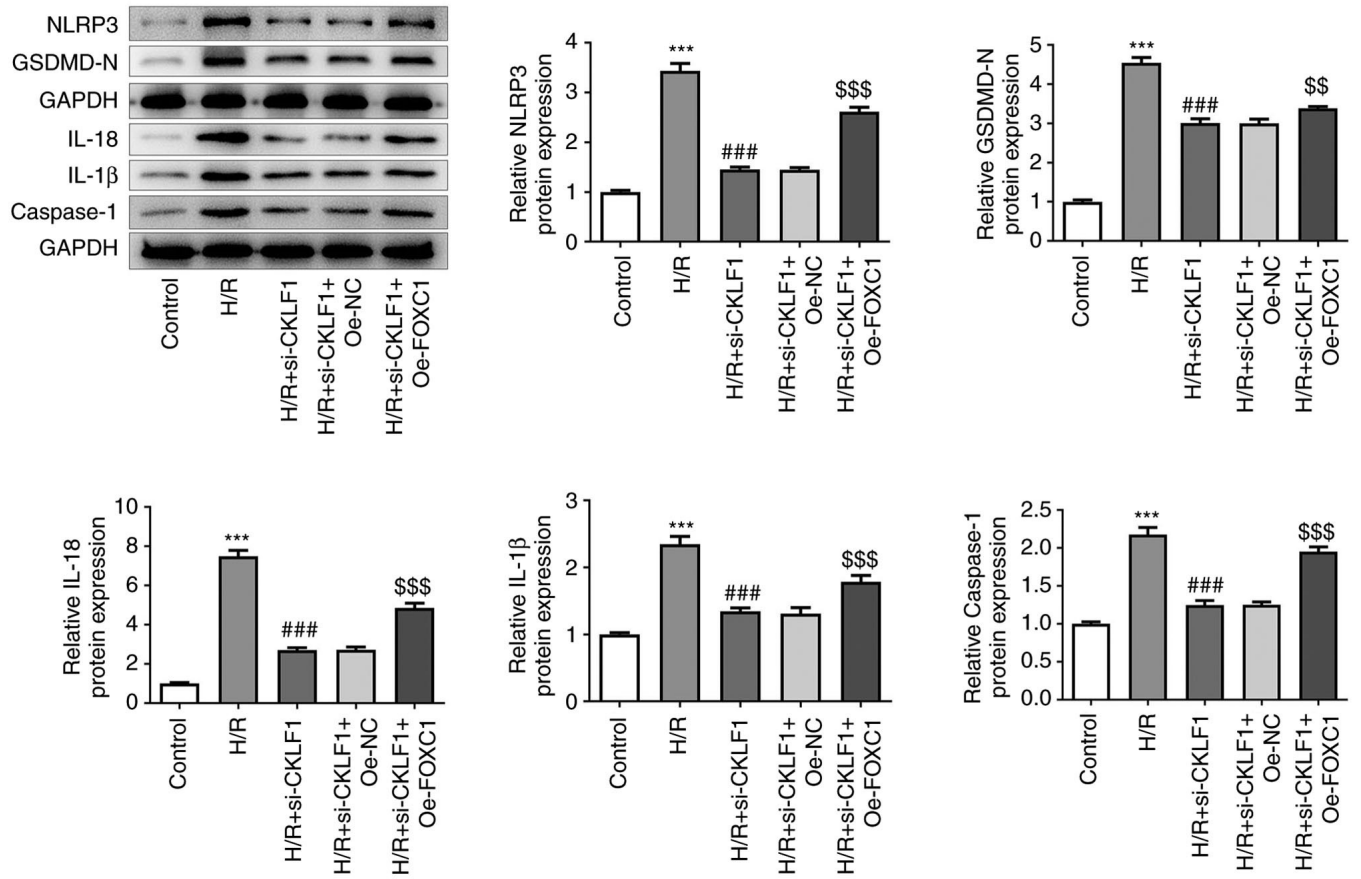

Figure 6. Oe-FOXC1 reverses the effects of CKLF1 knockdown on H/R-induced H9c2 cell damage via NLRP3 inflammasome signaling. The expression levels of proteins associated with NLRP3 inflammasome signaling were assessed by western blotting post-transfection with Oe-FOXC1 and si-CKLF1 in H9c2 cells exposed to H/R. ***P<0.001 vs. control; $^{###}$P<0.001 vs. H/R; $^{\$\$}$P<0.01, $^{\$\$\$}$P<0.001 vs. H/R + si-CKLF1 + Oe-NC. CKLF1, chemokine-like factor 1; FOXC1, forkhead box protein C1; GSDMD-N, gasdermin D N-terminal domain; H/R, hypoxia/reoxygenation; IL, interleukin; NC, negative control; NLRP3, NOD-like receptor family, pyrin domain containing 3; OE, overexpression; si, small interfering.

myocardial I/R injury and protect the myocardium (30). In addition, H/R-injured cardiomyocytes undergo processes, such as inflammatory reactions, which lead to the overproduction and excessive release of inflammatory factors, including TNF-α, IL-1β and IL-6 (31). Attenuating CKLF1-mediated inflammation, oxidative stress and apoptosis has been shown to exert protective effects on cisplatin-induced nephrotoxicity (24). Furthermore, CKLF1 is highly expressed during hepatic I/R, and CKLF1 inhibition attenuates neutrophil infiltration and reduces the inflammatory response to improve hepatic I/R injury (12). A previous study reported that IMM-H004 downregulates the levels of CKLF1 in adult and aged rats to inhibit the inflammatory response, and further protects from cerebral ischemia injury (32). The results of the present study suggested that knockdown of CKLF1 improved H/R-triggered oxidative stress and inflammation in H9c2 cells by decreasing the contents of ROS, MDA, TNF-α, IL-1β and IL-6, and increasing the activities of SOD and GSH-Px.

Using the JASPAR database, FOXC1 was identified as a putative transcription factor that can bind to the CKLF1 promoter. FOXC1 serves a significant role in the development of the heart and cardiovascular system, and abnormal FOXC1 function has been shown to be closely related to congenital heart disease and myocardial ischemia (16,33). Notably, FOXC1 expression can be induced by hypoxia and it can subsequently initiate inflammatory responses and cell injury (16). During myocardial I/R, FOXC1 has been reported to transcriptionally activate ELAVL1 to induce myocardial injury (34). Notably, suppressing FOXC1 expression exerts protective effects on human osteoarthritic synovial fibroblasts by inhibiting inflammation (35). Furthermore, endogenous ROS production in the early differentiation state of human cells inhibits endodermal differentiation via transient FOXC1 upregulation (36). In the present study, CKLF1 was identified as a novel target of FOXC1 via luciferase reporter and ChIP assays. FOXC1 directly bound to the CKLF1 promoter region to upregulate CKLF1 transcription and expression.

The NLRP3 inflammasome refers to a group of multimeric protein complexes consisting of NLRP3 and caspase 1, and is known to be associated with multiple cellular functions, including inflammation and apoptosis (37). Caspase 1 is the promoter of the NLRP3 inflammasome, which induces the production of mature IL-1β and IL-18 (38). Caspase 1 can also cleave GSDMD and generate GSDMD-N oligomers within the cell membrane, leading to disruption of the cell membrane integrity and promoting the release of cellular contents (39). H/R-induced upregulation of ROS production increases NLRP3 and caspase 1 expression, and promotes the release of pro-inflammatory cytokines (IL-18 and IL-1β) in rat cardiomyocytes (40). An increasing number of studies has validated

that suppression of the NLRP3 inflammasome can reduce myocardial infarct size and limit the inflammatory response following myocardial I/R in mice (41-43). Therefore, inhibition of NLRP3 inflammasome activation may help to mitigate myocardial I/R injury, and the NLRP3 inflammasome may thus be an important target for the prevention and treatment of myocardial I/R injury. Notably, IMM-H004 can downregulate the expression of CKLF1, thereby restraining activation of the NLRP3 inflammasome and subsequent inflammatory reaction, ultimately protecting the ischemic brain (11). Consistently, the present data showed that H/R led to the activation of NLRP3 inflammasome signaling, as evidenced by upregulated expression levels of NLRP3, GSDMD-N, IL-18, IL-1β and caspase 1 in H9c2 cells. CKLF1 silencing inhibited activation of the NLRP3 inflammasome, which was restored by FOXC1 overexpression.

In conclusion, to the best of our knowledge, this is the first report showing that CKLF1 expression is significantly increased in H/R-induced cardiomyocytes and CKLF1 knockdown plays inhibitory effects on H/R-triggered oxidative stress and inflammation. Mechanistically, CKLF1 could be transcriptionally activated by FOXC1 to aggravate H/R-induced damage of H9c2 cells by regulating NLRP3 inflammasome activation. These findings may provide new insights into the pathogenesis and treatment of myocardial I/R injury.

Acknowledgements

Not applicable.

Funding

No funding was received.

Availability of data and materials

The datasets used and/or analyzed during the current study are available from the corresponding author on reasonable request.

Authors' contributions

JP designed the study and drafted the manuscript. YJ analyzed the data, searched the literature and revised the manuscript. YJ and JP performed the experiments. JP and YJ confirm the authenticity of all the raw data. All authors have read and approved the final manuscript.

Ethics approval and consent to participate

Not applicable.

Patient consent for publication

Not applicable.

Competing interests

The authors declare that they have no competing interests.

References

1. Benjamin EJ, Virani SS, Callaway CW, Chamberlain AM, Chang AR, Cheng S, Chiuve SE, Cushman M, Delling FN, Deo R, *et al*: Heart disease and stroke statistics-2018 Update: A report from the american heart association. Circulation 137: e67-e492, 2018.
2. Jennings RB: Historical perspective on the pathology of myocardial ischemia/reperfusion injury. Circ Res 113: 428-438, 2013.
3. Gonzalez-Montero J, Brito R, Gajardo AI and Rodrigo R: Myocardial reperfusion injury and oxidative stress: Therapeutic opportunities. World J Cardiol 10: 74-86, 2018.
4. Kalogeris T, Baines CP, Krenz M and Korthuis RJ: Ischemia/Reperfusion. Compr Physiol 7: 113-170, 2016.
5. Mokhtari-Zaer A, Marefati N, Atkin SL, Butler AE and Sahebkar A: The protective role of curcumin in myocardial ischemia-reperfusion injury. J Cell Physiol 234: 214-222, 2018.
6. Han W, Lou Y, Tang J, Zhang Y, Chen Y, Li Y, Gu W, Huang J, Gui L, Tang Y, *et al*: Molecular cloning and characterization of chemokine-like factor 1 (CKLF1), a novel human cytokine with unique structure and potential chemotactic activity. Biochem J 357: 127-135, 2001.
7. Tan Y, Wang Y, Li L, Xia J, Peng S and He Y: Chemokine-like factor 1-derived C-terminal peptides induce the proliferation of dermal microvascular endothelial cells in psoriasis. PLoS One 10: e0125073, 2015.
8. Zhang T, Zhang X, Yu W, Chen J, Li Q, Jiao Y, He P and Shen C: Effects of chemokine-like factor 1 on vascular smooth muscle cell migration and proliferation in vascular inflammation. Atherosclerosis 226: 49-57, 2013.
9. Chen C, Chu SF, Ai QD, Zhang Z, Guan FF, Wang SS, Dong YX, Zhu J, Jian WX and Chen NH: CKLF1 aggravates focal cerebral ischemia injury at early stage partly by modulating Microglia/Macrophage toward M1 polarization through CCR4. Cell Mol Neurobiol 39: 651-669, 2019.
10. Kong LL, Wang ZY, Hu JF, Yuan YH, Han N, Li H and Chen NH: Inhibition of chemokine-like factor 1 protects against focal cerebral ischemia through the promotion of energy metabolism and anti-apoptotic effect. Neurochem Int 76: 91-98, 2014.
11. Ai QD, Chen C, Chu S, Zhang Z, Luo Y, Guan F, Lin M, Liu D, Wang S and Chen N: IMM-H004 therapy for permanent focal ischemic cerebral injury via CKLF1/CCR4-mediated NLRP3 inflammasome activation. Transl Res 212: 36-53, 2019.
12. Li FF, Zhou X, Chu SF and Chen NH: Inhibition of CKLF1 ameliorates hepatic ischemia-reperfusion injury via MAPK pathway. Cytokine 141: 155429, 2021.
13. Yang B, Hong T, Liu QZ, Feng XR, Gong YJ, Bu DF, Li XM, Xue L, Zhao CY and Huo Y: Effects of in vivo transfer of human chemokine-like factor 1 gene on cardiac function after acute myocardial infarction in rats. Beijing Da Xue Xue Bao Yi Xue Ban 41: 144-147, 2009 (In Chinese).
14. Feng XR, Hong T, Gong YJ, Bu DF, Yuan JY, Xue L, Zhao CY and Huo Y: In vivo transfer of human chemokine-like factor 1 gene increases peripheral blood CD34+ stem cells after myocardial infarction in rats. Beijing Da Xue Xue Bao Yi Xue Ban 38: 592-596, 2006 (In Chinese).
15. Lin YJ, Shyu WC, Chang CW, Wang CC, Wu CP, Lee HT, Chen LJ and Hsieh CH: Tumor hypoxia regulates forkhead box C1 to promote lung cancer progression. Theranostics 7: 1177-1191, 2017.
16. Zhang SP, Yang RH, Shang J, Gao T, Wang R, Peng XD, Miao X, Pan L, Yuan WJ, Lin L and Hu QK: FOXC1 up-regulates the expression of toll-like receptors in myocardial ischaemia. J Cell Mol Med 23: 7566-7580, 2019.
17. Zhao B, Li GP, Peng JJ, Ren LH, Lei LC, Ye HM, Wang ZY and Zhao S: Schizandrin B attenuates hypoxia/reoxygenation injury in H9c2 cells by activating the AMPK/Nrf2 signaling pathway. Exp Ther Med 21: 220, 2021.
18. Xu J, Huang J, He X, Hu M, Su S and Liu P: Myosin 1b Participated in the Modulation of Hypoxia/Reoxygenation-Caused H9c2 Cell Apoptosis and Autophagy. Anal Cell Pathol (Amst) 2022: 5187304, 2022.
19. Livak KJ, Schmittgen TD. Analysis of relative gene expression data using real-time quantitative PCR and the 2(-Delta Delta C(T)) method. Methods 25: 402-408, 2001.
20. Del Re DP, Amgalan D, Linkermann A, Liu Q and Kitsis RN: Fundamental mechanisms of regulated cell death and implications for heart disease. Physiol Rev 99: 1765-1817, 2019.

21. Badalzadeh R, Mokhtari B and Yavari R: Contribution of apoptosis in myocardial reperfusion injury and loss of cardioprotection in diabetes mellitus. J Physiol Sci 65: 201-215, 2015.
22. Zhang Q, Dang YY, Luo X, Fu JJ, Zou ZC, Jia XJ, Zheng GD and Li CW: Kazinol B protects H9c2 cardiomyocytes from hypoxia/reoxygenation-induced cardiac injury by modulating the AKT/AMPK/Nrf2 signalling pathway. Pharm Biol 61: 362-371, 2023.
23. Zhang Y, Wang Y, Ma Z, Liang Q, Tang X, Tan H, Xiao C and Gao Y: Ginsenoside Rb1 inhibits Doxorubicin-Triggered H9C2 cell apoptosis via aryl hydrocarbon receptor. Biomol Ther (Seoul) 25: 202-212, 2017.
24. Chen C, Ai Q and Wei Y: Hydroxytyrosol protects against cisplatin-induced nephrotoxicity via attenuating CKLF1 mediated inflammation, and inhibiting oxidative stress and apoptosis. Int Immunopharmacol 96: 107805, 2021.
25. Chen YE, Yang H, Pang HB and Shang FQ: Circ-CBFB exacerbates hypoxia/reoxygenation-triggered cardiomyocyte injury via regulating miR-495-3p in a VDAC1-dependent manner. J Biochem Mol Toxicol 36: e23189, 2022.
26. Yang H, Wang C, Zhang L, Lv J and Ni H: Rutin alleviates hypoxia/reoxygenation-induced injury in myocardial cells by up-regulating SIRT1 expression. Chem Biol Interact 297: 44-49, 2019.
27. Radak Z, Zhao Z, Goto S and Koltai E: Age-associated neurodegeneration and oxidative damage to lipids, proteins and DNA. Mol Aspects Med 32: 305-315, 2011.
28. Cadenas S: ROS and redox signaling in myocardial ischemia-reperfusion injury and cardioprotection. Free Radic Biol Med 117: 76-89, 2018.
29. Zhao Q, Liu Z, Huang B, Yuan Y, Liu X, Zhang H, Qiu F, Zhang Y, Li Y, Miao H, *et al*: PEDF improves cardiac function in rats subjected to myocardial ischemia/reperfusion injury by inhibiting ROS generation via PEDF-R. Int J Mol Med 41: 3243-3252, 2018.
30. Zhou T, Chuang CC and Zuo L: Molecular characterization of reactive oxygen species in myocardial Ischemia-Reperfusion Injury. Biomed Res Int 2015: 864946, 2015.
31. Algoet M, Janssens S, Himmelreich U, Gsell W, Pusovnik M, Van den Eynde J and Oosterlinck W: Myocardial ischemia-reperfusion injury and the influence of inflammation. Trends Cardiovasc Med 33: 357-366, 2023.
32. Ai Q, Chen C, Chu S, Luo Y, Zhang Z, Zhang S, Yang P, Gao Y, Zhang X and Chen N: IMM-H004 protects against cerebral ischemia injury and cardiopulmonary complications via CKLF1 mediated inflammation pathway in adult and aged rats. Int J Mol Sci 20: 1661, 2019.
33. Lambers E, Arnone B, Fatima A, Qin G, Wasserstrom JA and Kume T: Foxc1 regulates early cardiomyogenesis and functional properties of embryonic stem cell derived cardiomyocytes. Stem Cells 34: 1487-1500, 2016.
34. Chen HY, Xiao ZZ, Ling X, Xu RN, Zhu P and Zheng SY: ELAVL1 is transcriptionally activated by FOXC1 and promotes ferroptosis in myocardial ischemia/reperfusion injury by regulating autophagy. Mol Med 27: 14, 2021.
35. He X and Deng L: miR-204-5p inhibits inflammation of synovial fibroblasts in osteoarthritis by suppressing FOXC1. J Orthop Sci 27: 921-928, 2022.
36. Oka S, Tsuzuki T, Hidaka M, Ohno M, Nakatsu Y and Sekiguchi M: Endogenous ROS production in early differentiation state suppresses endoderm differentiation via transient FOXC1 expression. Cell Death Discov 8: 150, 2022.
37. Fouad AA, Abdel-Aziz AM and Hamouda AAH: Diacerein downregulates NLRP3/Caspase-1/IL-1beta and IL-6/STAT3 pathways of inflammation and apoptosis in a rat model of cadmium testicular toxicity. Biol Trace Elem Res 195: 499-505, 2020.
38. Bian Y, Li X, Pang P, Hu XL, Yu ST, Liu YN, Li X, Wang N, Wang JH, Xiao W, *et al*: Kanglexin, a novel anthraquinone compound, protects against myocardial ischemic injury in mice by suppressing NLRP3 and pyroptosis. Acta Pharmacol Sin 41: 319-326, 2020.
39. Shi H, Gao Y, Dong Z, Yang J, Gao R, Li X, Zhang S, Ma L, Sun X, Wang Z, *et al*: GSDMD-mediated cardiomyocyte pyroptosis promotes Myocardial I/R injury. Circ Res 129: 383-396, 2021.
40. Qiu Z, He Y, Ming H, Lei S, Leng Y and Xia ZY: Lipopolysaccharide (LPS) Aggravates High Glucose- and Hypoxia/Reoxygenation-Induced Injury through Activating ROS-Dependent NLRP3 Inflammasome-Mediated pyroptosis in H9C2 cardiomyocytes. J Diabetes Res 2019: 8151836, 2019.
41. Toldo S and Abbate A: The NLRP3 inflammasome in acute myocardial infarction. Nat Rev Cardiol 15: 203-214, 2018.
42. Wang Y, Yan X, Mi S, Li Z, Wang Y, Zhu H, Sun X, Zhao B, Zhao C, Zou Y, *et al*: Naoxintong attenuates Ischaemia/reperfusion Injury through inhibiting NLRP3 inflammasome activation. J Cell Mol Med 21: 4-12, 2017.
43. Toldo S, Marchetti C, Mauro AG, Chojnacki J, Mezzaroma E, Carbone S, Zhang S, Van Tassell B, Salloum FN and Abbate A: Inhibition of the NLRP3 inflammasome limits the inflammatory injury following myocardial ischemia-reperfusion in the mouse. Int J Cardiol 209: 215-220, 2016.